

## Enhanced mechanical properties of $\text{HfO}_2$ film by nitrogen doping

P. Lei, S. Guo, J. Zhu, B. Dai, G. Liu, Y. Wang & J. Han

**To cite this article:** P. Lei, S. Guo, J. Zhu, B. Dai, G. Liu, Y. Wang & J. Han (2016) Enhanced mechanical properties of  $\text{HfO}_2$  film by nitrogen doping, *Surface Engineering*, 32:8, 585-588, DOI: [10.1080/02670844.2015.1121342](https://doi.org/10.1080/02670844.2015.1121342)

**To link to this article:** <http://dx.doi.org/10.1080/02670844.2015.1121342>



Published online: 12 Feb 2016.



Submit your article to this journal 



Article views: 56



View related articles 



View Crossmark data 

# Enhanced mechanical properties of $\text{HfO}_2$ film by nitrogen doping

HPSTAR  
183-2016

P. Lei<sup>1</sup>, S. Guo<sup>1</sup>, J. Zhu<sup>\*1</sup>, B. Dai<sup>1</sup>, G. Liu<sup>2</sup>, Y. Wang<sup>3</sup> and J. Han<sup>1</sup>

The chemical composition, structure and mechanical properties of hafnium oxide films with different nitrogen constituents were investigated. X-ray photoelectron spectrum analysis showed that nitrogen atoms acted as oxygen substitution and interstitial atoms. The crystalline features exhibited no change during nitrogen doping. Nevertheless, the films with high compressive stress displayed significantly enhanced mechanical properties. The enhanced mechanism could mainly be attributed to the dislocation obstacle motion by inserting nitrogen atoms.

**Keywords:** Hafnium oxynitride film, Magnetron sputtering, Stress, Nitrogen doping, Hardness

## Introduction

Transition metal oxide/oxynitride thin films, due to the flexible constituent and promising properties, have attracted tremendous attention in both the scientific and technological communities over the past few years. Briefly, they could be applied to well-known tribological areas, including cutting tools and turbine blades because of super hardness and chemical stability;<sup>1</sup> they have been considered as optical coatings due to multispectral transmittance and low absorption,<sup>2</sup> and as promising insulating materials owing to high permittivity<sup>3</sup> and as ferroelectric materials.<sup>4</sup> As for the group of oxynitride materials, numerous researchers paid more attention on titanium oxynitride,<sup>5-7</sup> zirconium oxynitride,<sup>8,9</sup> hafnium oxynitride<sup>10,11</sup> and tantalum oxynitride.<sup>12,13</sup> Among them, hafnium oxynitride film has become one of the most fascinating films due to their peculiarly multifunctional properties.<sup>14-21</sup>

Various processes including reactive magnetron sputtering,<sup>15,22</sup> ion beam assisted deposition<sup>18</sup> and chemical vapour deposition<sup>16</sup> have been adopted to prepare hafnium oxynitride films. One of the most important and promising applications is the super mechanical properties of oxynitride films, which closely dependent on nitrogen content. However, it is difficult to obtain oxynitride films with a high fraction of nitrogen due to the strong and preferred O–M bond than N–M bond. To our best knowledge, studies regularly limited to the chemical composition, microstructure and mechanical properties of hafnium oxynitride films with different nitrogen contents.

In this work, we investigated the mechanical properties of hafnium oxynitride films with different nitrogen contents. Based on the characterisation of chemical composition and structures of films, the film stress and

mechanical properties have been measured and correlated to the intrinsic factors.

## Experimental details

The hafnium oxynitride films were prepared on Si(100) substrate by radio frequency magnetron sputtering using a metallic hafnium target (99.99% purity) with the reactive gas ratio of  $\text{N}_2/(\text{N}_2 + \text{O}_2)$  from 0.5 to 1. This reactive gas ratio can be realized by increasing the oxygen flow rate from 0 to 40 sccm and fixing the nitrogen gas flow at 40 sccm during deposition. Other growth parameters remained constant, including the argon flow rate of 50 sccm, the distance between target and substrate of 75 mm, the power of 120 W, and the total pressure of 1 Pa. The deposition time was 1 hour for all the samples, the film thickness varied from ~108 to 128 nm as the oxygen gas increases from 0 to 40 sccm during deposition.

High resolution X-ray photoelectron spectroscopy (XPS, PHI ESCA 5700) was used to determine the film composition with  $\text{Al K}\alpha$  radiation at 1486.6 eV. The structure was evaluated by GIXRD (X' Pert-Pro) with  $\text{Cu K}\alpha$  radiation source ( $\lambda = 1.541 \text{ \AA}$ ) at the incident angle of 1.5°. The stress of films was calculated by Stoney equation, using the curvature and thickness measured by profilometry. The hardness and elastic modulus of the films were evaluated by Nanoindenter XP with continuous stiffness measurement mode. This instrument monitors and records the dynamic load and displacement of the three-sided pyramidal diamond (Berkovich) indenter with a tip radius of about 40 nm during indentation with a force resolution of about 50 nN and displacement resolution of about 0.1 nm. The indentation depth is 430 nm for each sample. The hardness and modulus values were chosen as the real hardness and modulus of films when the indentation depth is in the around 10 times less than film thickness.

## Discussion and results

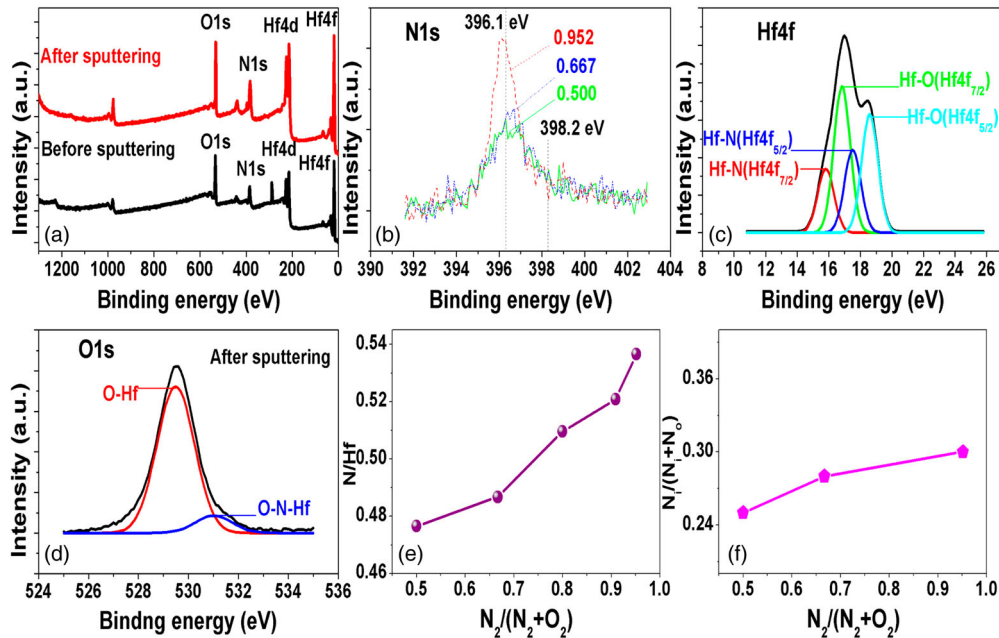
The composition and chemical bonds of as-deposited films were evaluated by XPS, which are shown in Fig. 1.

<sup>1</sup>Center for Composite Materials, Harbin Institute of Technology, PR China

<sup>2</sup>Center for High Pressure Science and Technology Advanced Research, Shanghai 201203, PR China

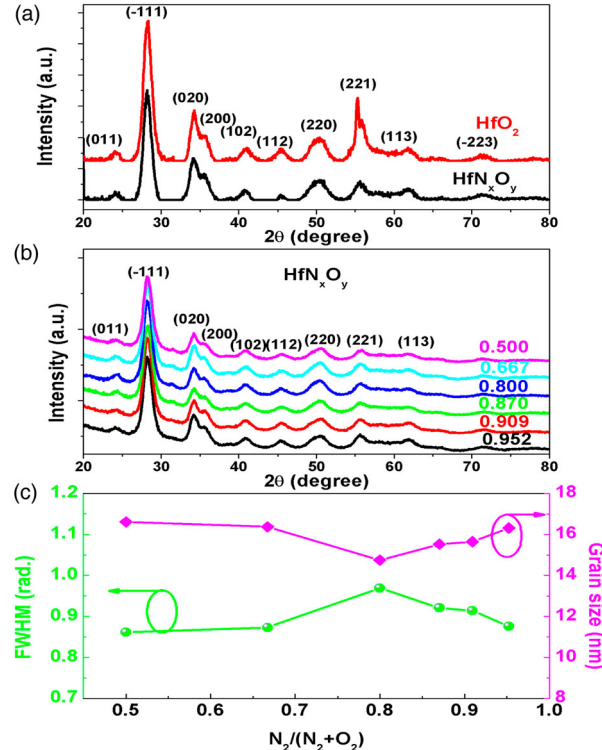
<sup>3</sup>Institute of Electronic Engineering, China Academy of Engineering Physics, Mianyang 621999, PR China

\*Corresponding author, email zhujq@hit.edu.cn



1 The survey XPS spectra of films at  $\text{N}_2/(\text{N}_2 + \text{O}_2)$  ratio of 0.952 before and after sputtering a; the core level of N1s spectra of films at  $\text{N}_2/(\text{N}_2 + \text{O}_2)$  ratio of 0.5, 0.667 and 0.952 after sputtering b; the core level spectra of Hf4f at the ratio of 0.952 c; the core level spectra of O1s of films at the ratio of 0.87 d; the ratio of e N/Hf and f  $\text{N}/(\text{N}_i + \text{N}_o)$  as a function of  $\text{N}_2/(\text{N}_2 + \text{O}_2)$  ratio

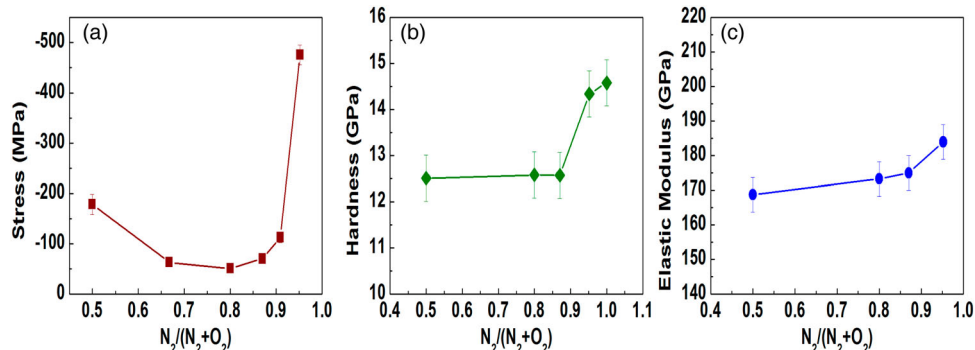
Figure 1a exhibits the survey spectra of films at  $\text{N}_2/(\text{N}_2 + \text{O}_2)$  of 0.952 before and after argon ions sputtering for 5 minutes. It is clear that the strong peaks come from N, O, Hf and the adventitious elements exist in the films regardless of sputtering. Figure 1b displays the XPS spectra of N1s at different  $\text{N}_2$  flow rates after sputtering for 5 minutes. The nitrogen content increases in the films as the nitrogen gas increases. Due to 5 minutes sputtering and etching, absorbed nitrogen from the exposed air has a slight influence on film composition. According to GIXRD patterns (see Fig. 2), there is no peaks from HfN phase, meaning no HfN phase formation as the nitrogen increases. Thus, it is reasonably speculated that the nitrogen exists in two chemical states, i.e. interstitial one (expressed as  $\text{N}_i$ ) and substituted one (expressed as  $\text{N}_o$ ). According to the asymmetry of N1s peak, the N1s peak can be deconvoluted into two peaks located at 396.1 eV and 398.2 eV, corresponding to Hf–N–Hf bond ( $\text{N}_i$ ) and Hf–N–O bond ( $\text{N}_o$ ),<sup>23</sup> which is similar to the nitrogen doping yttrium oxide and titanium oxide films.<sup>24,25</sup> The N1s binding energy of the latter site is about 2 eV higher than that of the former due to more negative charge of N residing in the latter site. The spectra of Hf4f core level were shown in Fig. 1c. The Hf4f can be deconvoluted into two doublet peaks due to the spin-orbit splitting (Hf4f7/2 and Hf4f5/2), the first pair is located at 15.8 and 17.5 eV corresponding to the Hf–N bond,<sup>10</sup> it shifts to a higher binding energy by ~0.5 compared with the reported Hf–N bonding energy,<sup>26</sup> the others are located at 16.8 and 18.4 eV in consistence with Hf–O bond, which shifts a lower binding energy compared with Hf–O binding energy in  $\text{HfO}_2$  films.<sup>10,27</sup> The shift of binding energy is due to the nitrogen incorporation into the films, which has confirmed the nitrogen bonds again. Similarly, the spectra of O1s of films at nitrogen flow ratio of 0.8 reveal the trend as shown in the Fig. 1d. The nitrogen incorporation causes the lower shift of



2 The GIXRD patterns of a  $\text{HfN}_x\text{O}_y$  films at the  $\text{N}_2$  flow rate of 0 and 40 sccm and b  $\text{HfN}_x\text{O}_y$  films as a function of  $\text{N}_2/(\text{N}_2 + \text{O}_2)$  ratio; c the FWHM and grain size of films as a function of  $\text{N}_2/(\text{N}_2 + \text{O}_2)$  ratio

Hf–O bond due to the more negative charge.<sup>28</sup> The peak (~531.1 eV) is believed to be the Hf–N–O bond.

The calculated ratio of N/Hf is plotted in Fig. 1e, as the ratio increases, the ratio of N/Hf increases from 0.48 to



3 The stress *a*, the hardness *b* and modulus *c* of  $\text{HfN}_x\text{O}_y$  films as a function of  $\text{N}_2/(\text{N}_2 + \text{O}_2)$  ratio

0.54, indicating that the N content increases in the films. For the variation of  $\text{N}_i$  and  $\text{N}_o$  as the nitrogen content increases, Fig. 1*f* gives the ratio of interstitial N atoms to the total N atoms, showing the increased tendency and indicating more content of interstitial N in films at higher nitrogen atmosphere.

Figure 2*a* shows the crystalline structures of films prepared at  $\text{N}_2$  flow rate of 0 and 40 sccm corresponding to  $\text{HfO}_2$  film and  $\text{HfN}_x\text{O}_y$  film. There is no  $\text{HfN}$  phase formation. Such interstitial N and other substituted N cannot change the Hf–N bonds arrangement to form  $\text{HfN}$  phase due to the similar radius between N and O atoms. Consequently, the GIXRD patterns of  $\text{HfN}_x\text{O}_y$  films at different rates from 0.5 to 0.925 show the same case (in Fig. 2*b* and *c*). The structural stability through incorporating nitrogen is also verified by theoretical calculation.<sup>29</sup>

The residual stress of films was calculated by Stoney equation through measuring the film thickness and the curvature of film-substrate by profilometry.<sup>30</sup> The modulus and Poisson's ratio of silicon substrate are 202 GPa and 0.27, respectively. All the deposited films have compressive stress. Figure 3*a* shows the stress of films grown at different  $\text{N}_2/(\text{N}_2 + \text{O}_2)$  ratios, which is in the level of MPa. As the reactive nitrogen gas increases, the stress first slightly decreases to  $\sim 50$  MPa, and subsequently abruptly increase occurs to 478 MPa. The compressive stress of films is generally recognised to be originated from energetic particles bombardment during film deposition.<sup>31</sup> In this work, the nitrogen incorporation mainly plays a role especially from the interstitial N atoms. The deposited films are polycrystalline; the N interstitial atoms could take up in grains and grain boundaries. Nitrogen atoms favourably arrange in boundaries, because the weak reactivity and the relief of defects.<sup>32</sup> Therefore, with the increase of nitrogen atoms in films, the interstitial nitrogen atoms cause large compressive once larger than the threshold shown in Fig. 3*a*.

Figure 3*b* and *c* displays the hardness and modulus of  $\text{HfN}_x\text{O}_y$  films. It is clear to observe that the hardness maintains a lower constant ( $\sim 12.5$  GPa), when the  $\text{N}_2/(\text{N}_2 + \text{O}_2)$  ratio reaches at 0.925, the hardness abruptly increases up to 14.5 GPa in Fig. 3*b*. In this work, nitrogen content and stress are the dominant change. It seems that the nitrogen content and accordingly high stress contribute the enhanced hardness. Indeed, several reports have showed the similar correlation between stress and hardness in  $\text{TiN}_x\text{O}_y$  films,<sup>33</sup> N doped WC films<sup>34</sup> and  $\text{TiN}_{x-1}\text{C}_{1-x}$  films.<sup>35</sup> The incorporated nitrogen in films could contribute the strengthened hardness. The

substituted atoms (the N–Hf bond) has more covalent than O–Hf and thus has strong bond energy,<sup>36</sup> while it has less influence on stress. However, the interstitial atoms mainly exist in grain boundaries, giving rise to pronounced strain hardening results, which acts as an obstacle for dislocation motion.<sup>33,35,37–39</sup> The elastic modulus of such material is proportional to that of the hardness according to the Griffith theory.<sup>40</sup>

## Conclusion

Nitrogen doped hafnium oxynitride films were realised by R.F. magnetron sputtering at the mixture atmosphere (oxygen and nitrogen). The composition and chemical bonds of HfON films were determined by XPS. Nitrogen content increases with the input nitrogen gas and the nitrogen atoms show the interstitial and substituted atoms in the films. Although nitrogen doping has no influences on the structures, the stress measurements indicate the obvious relation to the nitrogen contents. The enhanced hardness can be obtained at high concentration nitrogen doping. The increasingly distorted energy by interstitial nitrogen mainly contributes the largely enhanced hardness of  $\text{HfN}_x\text{O}_y$  films. This present work can provide the useful guide for engineering applications.

## Acknowledgements

This work was supported by National Natural Science Excellent Young Foundation of China (Grant No. 51222205) and the National Natural Science Foundation of China (Grant No. 51372053).

## References

1. J. Nohava, P. Dessarzin, P. Karvankova and M. Morstein: 'Characterization of tribological behavior and wear mechanisms of novel oxynitride PVD coatings designed for applications at high temperatures', *Tribol. Int.*, 2015, **81**, 231–239.
2. D. Cristea, D. Constantin, A. Crisan C. S. Abreu, J. R. Gomes, N. P. Barradas, E. Alves, C. Moura, F. Vaz and L. Cunha: 'Properties of tantalum oxynitride thin films produced by magnetron sputtering: The influence of processing parameters', *Vacuum*, 2013, **98**, (11), 63–69.
3. H.-S. Kim, S. H. Jeon, J. S. Park, T. S. Kim, K. S. Son, J.-B. Seon, S.-J. Seo, S.-J. Kim, E. Lee, J. G. Chung, K. Lee, S. Han, M. Ryu, S. Y. Lee and K. Kim: 'Anion control as a strategy to achieve high-mobility and high-stability oxide thin-film transistors', *Sci. Rep.*, 2013, **3**, (1459), 1–7.
4. D. Oka, Y. Hirose, H. Kamisaka, T. Fukumura, K. Sasa, S. Ishii, H. Matsuzaki, Y. Sato, Y. Ikuhara and T. Hasegawa: 'Possible

ferroelectricity in perovskite oxynitride  $\text{SrTaO}_2\text{N}$  epitaxial thin films', *Sci. Rep.*, **2014**, *4*, 4987.

5. R. Asahi and T. Morikawa: 'Nitrogen complex species and its chemical nature in  $\text{TiO}_2$  for visible-light sensitized photocatalysis', *Chem. Phys.*, **2007**, *339*, 57–63.
6. E. Çetinörgü-Goldenberg, L. Burstein, I. Chayun-Zucker, R. Avni and R. L. Boxman: 'Structural and optical characteristics of filtered vacuum arc deposited  $\text{N}: \text{TiO}_x$  thin films', *Thin Solid Films*, **2013**, *537*, 28–35.
7. A. S. Bolokang, D. E. Motaung, C. J. Arendse and T. F. G. Muller: 'Formation of faced-centered cubic and tetragonal titanium oxynitride by low temperature annealing of ball milled titanium powder in air', *Adv. Powder. Technol.*, **2015**, *26*, 167–175.
8. M. J. Pinzón, J. E. Alfonso, J. J. Olaya, G. I. Cubillos and E. Romero: 'Influence of the electrical power applied to the target on the optical and structural properties of  $\text{ZrON}$  films produced via RF magnetron sputtering in a reactive atmosphere', *Thin Solid Films*, **2014**, *572*, 184–188.
9. G. I. Cubillos, M. Bethencourt and J. J. Olaya: 'Corrosion resistance of zirconium oxynitride coatings deposited via DC unbalanced magnetron sputtering and spray pyrolysis-nitriding', *Appl. Surf. Sci.*, **2015**, *327*, 288–295.
10. C. S. Kang, H.-J. Cho, K. Onishi, R. Nieh, R. Choi, S. Gopalan, S. Krishnan, J. H. Han and J. C. Lee: 'Bonding states and electrical properties of ultrathin  $\text{HfO}_x\text{N}_y$  gate dielectrics', *Appl. Phys. Lett.*, **2002**, *81*, 2593–2595.
11. J. F. Kang, H. Y. Yu, C. Ren, M.-F. Li, D. S. H. Chan, H. Hu, H. F. Lim, W. D. Wang, D. Gui and D.-L. Kwong: 'Thermal stability of nitrogen incorporated in  $\text{HfN}_x\text{O}_y$  gate dielectrics prepared by reactive sputtering', *Appl. Phys. Lett.*, **2004**, *84*, 1588–1590.
12. J. Rezek, J. Vlček, J. Houška and R. Čerstvý: 'High-rate reactive high-power impulse magnetron sputtering of  $\text{Ta}-\text{O}-\text{N}$  films with tunable composition and properties', *Thin Solid Films*, **2014**, *566*, 70–77.
13. E. Nurlaela, M. Harb, S. Gobbo, M. Vashishta and K. Takanabe: 'Combined experimental and theoretical assessments of the lattice dynamics and optoelectronics of  $\text{TaON}$  and  $\text{Ta}_3\text{N}_5$ ', *J. Solid State Chem.*, **2015**, *229*, 219–227.
14. M. Liu, Q. Fang, G. He, L. Zhu and L. Zhang: 'Characterization of  $\text{HfO}_x\text{N}_y$  gate dielectrics using a hafnium oxide as target', *Appl. Surf. Sci.*, **2006**, *252*, 8673–8676.
15. X. M. Cai, F. Ye, E. Q. Xie, D. P. Zhang and P. Fan: 'Effect of  $\text{N}_2$  ambient annealing on the field emission properties of  $\text{HfN}_x\text{O}_y$  thin films', *Appl. Phys. A*, **2008**, *90*, 555–558.
16. Q. Luo, D. W. Hess and W. S. Rees Jr.: 'Effect of oxidant on downstream microwave plasma-enhanced CVD of hafnium oxynitride films', *Chem. Vapor Depos.*, **2006**, *12*, 181–186.
17. M. Liu, Q. Fang, G. He, L. Li, L. Q. Zhu, G. H. Li and L. D. Zhang: 'Effect of post deposition annealing on the optical properties of  $\text{HfO}_x\text{N}_y$  films', *Appl. Phys. Lett.*, **2006**, *88*, 192904.
18. Y. Wang, J. Zhang, F. Zhang, F. Zhang and S. Zou: 'Field emission from hafnium oxynitride films prepared by ion beam-assisted deposition', *Appl. Surf. Sci.*, **2005**, *242*, 407–411.
19. G. He, Q. Fang and L. D. Zhang: 'Structural and interfacial properties of high- $k$   $\text{HfO}_x\text{N}_y$  gate dielectric films', *Mater. Sci. Semicond. Process.*, **2006**, *9*, 870–875.
20. L. Yuan, G. Fang, H. Zhou, Y. Gao, C. Liu and X. Zhao: 'Suppression of near-edge optical absorption band in sputter deposited hafnium oxynitride via nitrogen incorporation and annealing', *J. Phys. D Appl. Phys.*, **2009**, *42*, 145302.
21. S. Venkataraj, D. Severin, S. H. Mohamed, J. Ngaruuya, O. Kappertz and M. Wuttig: 'Towards understanding the superior properties of transition metal oxynitrides prepared by reactive DC magnetron sputtering', *Thin Solid Films*, **2006**, *502*, 228–234.
22. X.-M. Cai, F. Ye, E.-Q. Xie, D.-P. Zhang and P. Fan: 'Field electron emission from  $\text{HfN}_x\text{O}_y$  thin films deposited by direct current sputtering', *Appl. Surf. Sci.*, **2008**, *254*, 3074–3077.
23. K. Ramani, C. R. Essary, V. Craciun and R. K. Singh: 'UV assisted oxidation and nitridation of hafnia based thin films for alternate gate dielectric applications', *Appl. Surf. Sci.*, **2007**, *253*, 6493–6498.
24. Z. M. Liu, L. Y. Liang, Z. Yu, S. K. He, X. J. Ye, X. L. Sun, A. H. Sun and H. T. Cao: 'Structural and electrical characteristics of RF sputtered YON gate dielectrics and their thin-film transistor applications', *J. Phys. D Appl. Phys.*, **2011**, *44*, 155403.
25. Z. Zhou and Y. Huang: 'The stable and uniform characteristics of nitrogen in nitrogen doped titanium dioxide nano photocatalytic particles', *J. Phys. Conf. Ser.*, **2009**, *188*, 012033.
26. P. D. Kirsch, C. S. Kang, J. Lozano, J. C. Lee and J. G. Ekerdt: 'Electrical and spectroscopic comparison of  $\text{HfO}_2/\text{Si}$  interfaces on nitrided and un-nitrided  $\text{Si}(100)$ ', *J. Appl. Phys.*, **2002**, *91*, 4353–4363.
27. C. Morant, L. Galan and J. M. Sanz: 'An XPS study of the initial stages of oxidation of hafnium', *Surf. Interface Anal.*, **1990**, *16*, 304–308.
28. G. He, M. Liu, L. Q. Zhu, M. Chang, Q. Fang and L. D. Zhang: 'Effect of postdeposition annealing on the thermal stability and structural characteristics of sputtered  $\text{HfO}_2$  films on  $\text{Si}(100)$ ', *Surf. Sci.*, **2005**, *576*, 67–75.
29. M. Saitoh, T. Mizoguchi, T. Tohei and Y. Ikuhara: 'First principles calculation of dopant solution energy in  $\text{HfO}_2$  polymorphs', *J. Appl. Phys.*, **2012**, *112*, 084514.
30. B. K. Gan, M. M. M. Bilek, D. R. McKenzie, M. B. Taylor and D. G. McCulloch: 'Effect of intrinsic stress on preferred orientation in  $\text{AlN}$  thin films', *J. Appl. Phys.*, **2004**, *95*, 2130–2134.
31. J. A. Thornton and D. W. Hoffman: 'Stress-related effects in thin films', *Thin Solid Films*, **1989**, *171*, 5–31.
32. G. He, L. D. Zhang, G. H. Li, M. Liu, L. Q. Zhu, S. S. Pan and Q. Fang: 'Spectroscopic ellipsometry characterization of nitrogen-incorporated  $\text{HfO}_2$  gate dielectrics grown by radio-frequency reactive sputtering', *Appl. Phys. Lett.*, **2005**, *86*, 232901.
33. F. Vaz, P. Cerqueira, L. Rebouta, S. M. C. Nascimento, E. Alves, Ph. Goudeau, J. P. Rivière, K. Pischow and J. De Rijk: 'Structural, optical and mechanical properties of coloured  $\text{TiN}_x\text{O}_y$  thin films', *Thin Solid Films*, **2004**, *447–448*, 449–454.
34. Y. D. Su, C. Q. Hu, C. Wang, M. Wen and W. T. Zheng: 'Relatively low temperature synthesis of hexagonal tungsten carbide films by N doping and its effect on the preferred orientation, phase transition, and mechanical properties', *J. Vac. Sci. Technol. A*, **2009**, *27*, 167–173.
35. L. Karlsson, L. Hultman and J.-E. Sundgren: 'Influence of residual stresses on the mechanical properties of  $\text{TiC}_x\text{N}_{1-x}$  ( $x = 0, 0.15, 0.45$ ) thin films deposited by arc evaporation', *Thin Solid Films*, **2000**, *371*, 167–177.
36. F. Gao, J. He, E. Wu, S. Liu, D. Yu, D. Li, S. Zhang and Y. Tian: 'Hardness of covalent crystals', *Phys. Rev. Lett.*, **2003**, *91*, 015502.
37. J. Xu, Z. Y. Li, Z.-H. Xie and P. Munroe: 'Uniting superhardness and damage-tolerance in a nanosandwich-structured Ti–B–N coating', *Scr. Mater.*, **2014**, *74*, 88–91.
38. O. Banakh, P. A. Steinmann and L. Dumitrescu-Buform: 'Optical and mechanical properties of tantalum oxynitride thin films deposited by reactive magnetron sputtering', *Thin Solid Films*, **2006**, *513*, (1–2), 136–141.
39. F. Vaz, P. Carvalho, L. Cunha, L. Rebouta, C. Moura, E. Alves, A. R. Ramos, A. Cavaleiro, Ph. Goudeau and J. P. Rivière: 'Property change in  $\text{ZrN}_x\text{O}_y$  thin films: effect of the oxygen fraction and bias voltage', *Thin Solid Films*, **2004**, *469–470*, 11–17.
40. M. Ohring: 'Materials science of thin films: deposition and structure', 2nd edn; **2002**, Hoboken, NJ, Academic Press.